SLAC PROPOSAL E-163
August 24, 2001

Laser Acceleration of Electrons in Vacuum

C. D. Barnes, E. R. Colby*, B. M. Cowan, R. J. Noble,
D. T. Palmer, R. H. Siemann, J. E. Spencer, D. R. Walz

Stanford Linear Accelerator Center

R. L. Byer, T. Plettner

Stanford University

Abstract

Laser-powered acceleration of charged particles promises extraordinary acceleration gradients due to the immense power available from lasers. This possibility has led to many proposed structures for laser acceleration; however, the field of vacuum laser acceleration is almost wholly unexplored experimentally. Recent advances in laser efficiency and phase synchronization have made possible a practical laser accelerator and are a strong motivation for this experiment.

We propose to investigate the physical mechanism and technical viability of laser linear acceleration in vacuum. We propose to experimentally test electron bunching at optical wavelengths, a key step in developing particle sources for laser accelerators, and to devise and test lithographic structures suitable for staged laser acceleration. This proposal is part of a larger research effort including efficient mode-locked laser development and advanced lithographic structure development.

We request some modifications to the NLCTA (Next Linear Collider Test Accelerator) and the construction of a small facility for performing laser acceleration experiments.

* Spokesman

Overview

The rapid increase in center-of-mass energies and luminosities available at colliders has led to a wealth of exciting and fundamental discoveries in particle physics. What has driven this progress has been sustained research to improve existing accelerators, and to invent new acceleration techniques. By the end of this decade, the tools at the energy frontier of accelerator-based high energy physics are expected to be the LHC and a complementary lepton collider of 0.5 TeV center of mass energy. What machines will or can succeed these machines is far from clear.

What is clear is that the physics questions will be no less momentous. As Michael Peskin recently observed:

> Depending on what is found at these machines the possibilities for the future branch out in different directions:
>
> - The LHC and LC experiments may discover supersymmetric particles. In this case, the LHC will discover some or all of the supersymmetry partners of quarks and gluons, while the LC will make a detailed study of the Higgs boson and the partners of the photon, W, and Z. It is possible that the partners of the leptons will be too heavy to pair-produce at a 1 TeV e+e- collider, and it is likely that the partners of quarks will not be seen at such a machine. Studies at higher energies will make precise measurements of the properties of these particles. In addition, if the BaBar and BELLE experiments discover that CP violation cannot be accounted for within the Standard Model, the most likely new source is flavor-mixing of squarks that would be directly probed in these experiments.
>
> - The LHC and LC experiments may discover strong interactions of the top quark responsible for electroweak symmetry breaking. In this case, an e+e- collider of multi-TeV energy would be expected to pair-produce excited states or other partners of the top quark, and also very heavy top-antitop resonances that would reveal the basic structure of the new interactions.
>
> - The LHC and LC experiments may discover large extra space dimensions. In this case, e+e- experiments at multi-TeV energies may reveal the spectrum of resonances regularly spaced in mass-squared characteristic of string theory. At higher energies, the cross section of e+e- annihilation becomes dominated by black hole production.

Machines capable of reaching the center-of-mass energies needed for these inquiries take significant time to develop. Research on technologies for these machines must proceed in parallel with the development of the next colliders if it is to reach sufficient maturity for timely construction of the subsequent generation of machines. Obtaining higher acceleration gradients is key to reaching higher energies economically. A significant improvement in gradient not only will save on physical length and cost, but will likely result in a reduction in the number of components, with the gain in reliability being potentially significant.

It is also highly desirable that future accelerators be assembled from technologies that enjoy large markets for the obvious reason that strong market forces drive aggressive research and development, which lowers cost and improves quality. Both lasers and semiconductors enjoy large markets.

"Starting from the 1930s, accelerator energy has increased--by about a factor of 10 every six to eight years…this spectacular achievement has resulted from a succession of technologies rather than from construction of bigger and better machines of a given type." W. K. H. Panofsky, 1997

Motivation

Demands of high-energy physics are such that achieving the highest possible energy gain in a given distance is of paramount importance if a linear collider beyond the NLC is to be economically feasible. This in turn requires coherent radiation sources capable of very high peak power for short pulses, traditionally a role played by klystrons in microwave accelerators. Laser acceleration has the potential for extremely high gradient, deriving from two advantages lasers have over microwave tubes as power sources for a linear collider. First, considerably higher peak powers are possible with lasers. For instance, a commercially available Ti:Sapphire laser can produce a peak power of 10 GW at 0.8 micron versus 75 MW at 11.4 GHz from the SLAC X-band klystron.

Second, there is significant industry interest in developing higher power laser sources and power handling devices at a time when industry interest in vacuum power tubes is declining. The extraordinary growth in the use of the Internet has driven the telecommunications industry to what analysts predict will soon be a trillion-dollar-a-year market. Explosive growth of fiber optic networks for long-haul data transmission is driving the development of inexpensive lasers and associated technologies, including lithographically produced optical components. As an example, phase locking of a mode-locked femtosecond laser to a CW reference has been recently accomplished,[1] and is being actively pursued at NIST in efforts to develop an optical frequency comb for use as a measurement standard.[2] This represents a critical step toward powering multiple accelerator structures. Highly efficient lasers are also being developed, with solid state lasers at longer wavelengths producing wall-plug-to-photon efficiencies of 20% or better (e.g. Cr^{++}:ZnSe, 20%[3]; Yb:$KGd(WO_4)_2$, 28%[4]; Yb:$KY(WO_4)_2$, 40%[5]). Developing acceleration methods that will capitalize on inexpensive, efficient power sources and components is therefore very attractive economically, and is rapidly becoming feasible technically.

Industry interest also includes microstructure development, raising the possibility of inexpensively producing highly complex accelerating structures. Structure fabrication is critical to laser acceleration, since a key difficulty in developing accelerator technologies suited to laser sources derives from the short wavelengths at which the most efficient, commercially viable lasers operate. Traditional metallic accelerating structures composed of disk-loaded circular waveguides when operated in the lowest passband simply become too difficult to fabricate at optical wavelengths due to prohibitively tight tolerances. Further, such structures would not survive the intense surface heating when powered. Consequently, new concepts capable of efficiently coupling coherent radiation to a passing particle beam must be sought out and tested.

Numerous schemes have been proposed for coupling laser energy to charged particle beams, covering structures that are dielectric, metallic, or plasma, and coupling to the beam in both far-field (plane-wave like fields) and near-field (fields near a focus). We propose to investigate near-field dielectric structures for several reasons. Dielectric

reflectors, composed of many quarter-wave thick layers or a chemically etched graded index coating on a substrate, tolerate typically an order-of-magnitude higher fluences (power per unit area) than highly polished metallic surfaces of any kind. This superior damage resistance permits significantly higher accelerating gradients. Ultimately, however the requirement to make thousands of sub-micron accuracy structures of the scale ~100λ motivates us to consider lithography for a future collider.

The prospect of producing highly complex dielectric accelerating structures with submicron dimensional accuracy inexpensively would be formidable were it not already a matter of routine in the semiconductor industry. The fundamental question for accelerator applications is whether high damage threshold materials can be lithographically processed. Since the optical material $Si0_2$ (silica) is already routinely lithographically etched in semiconductor processing, and Si itself is transparent at wavelengths longer than 1.0 μm, this is expected to be a matter of material science, not fabrication. Additionally, the recent and aggressive pursuit of CVD diamond films in chip production offers the possibility of still higher damage threshold materials with excellent thermal properties. The optimal wavelength choice will be defined by the mutually overlapping capabilities of efficient lasers, high-damage-threshold materials amenable to lithography, and the future direction of the telecom industry, and will likely fall in the 1.0-2.0 μm range. The availability of commercial well-engineered Ti:Sapphire lasers has led to our present work at 0.8 μm where the issues are the same as at the slightly longer wavelengths.

The goal is to lithographically produce the power source, power transmission system, accelerator structures and beam diagnostics on a single substrate by semiconductor process. When this is achieved, the complexity of the structures will no longer be a major cost factor, the number of components requiring hand assembly into a working accelerator will be reduced, and the cost and reliability will be greatly improved.

Theory

The production of a synchronous, axially-directed electric field with a minimum of boundaries and materials on or near the beam path is the principle physics consideration for any accelerator structure. Power efficiency and construction from materials that have good resistance to damage from the accelerating fields and radiation, are easily fabricated, and are inexpensive are the principle technical considerations. In addition, the basic accelerating method should be scalable to very high energies.

A scheme proposed by Pantell and Piestrup[6] with a conceptual modification by Haarland[7] offers all of the desired physical characteristics and many of the technical characteristics. Two linearly polarized Gaussian beams are crossed at a small angle to the electron beam axis and focused at the crossing point. The laser fields must be terminated (by striking a reflecting surface which diverts the laser pulses away from the electron bunch) in order to give net energy gain. The transverse field components cancel if the waves are out of phase by π, and the resultant axially-directed component gives energy gain to the electron beam over very large distances ($\sim 10^3$ λ) before another boundary must be interposed. This is in marked contrast to traditional microwave accelerators, for which boundaries must be placed at distances less than a wavelength apart, and permits laser accelerating structures to have dimensions of order millimeters, rather than microns.

The focusing of the laser implies that the fluence on the boundaries is somewhat reduced thereby enhancing damage resistance. Finally, the simple geometry required to produce this field configuration is amenable both to lithographic production, and to construction out of conventional optical components, permitting straightforward construction of a prototype.

Figure 1 shows a realization of this acceleration scheme using two prisms and two high reflectors bonded to form a vee-shaped acceleration region. The two laser pulses are incident from above, reflect from prisms into the horizontal direction, and co-propagate with the electron beam through the cell. The optical fields are reflected backwards (not shown) by the downstream high reflectors, and bounce back out of the cell vertically (also not shown). The reflected pulses are not synchronous with the electron beam and have negligible effect on the energy gain.

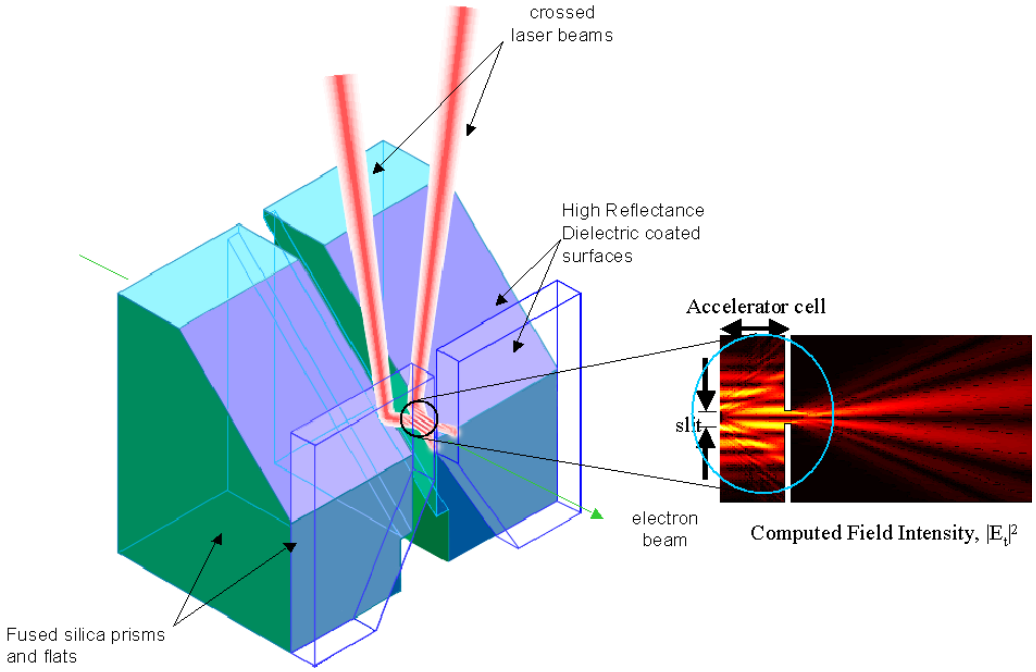

FIGURE 1: The vacuum laser acceleration cell and computed electric field distribution.

Openings must be made in the accelerator cell for the electron beam to pass, which modifies the fields inside the cell. Numerical calculation of the field distribution, outlined in Appendix A and shown in Figure 1 above, shows that the acceleration fields "leak out" behind the downstream reflecting surfaces, diffracting away rapidly. These leakage fields, in contrast to the reverse reflection fields, are synchronous and appreciably lower the energy gain if the slits are opened too wide, much as opening the irises of a conventional microwave structure leads to reduced accelerating fields. The decelerating nature of these fields and resultant decrease in energy gain, computed for 100 fsec long laser pulses, is illustrated in Figure 2.

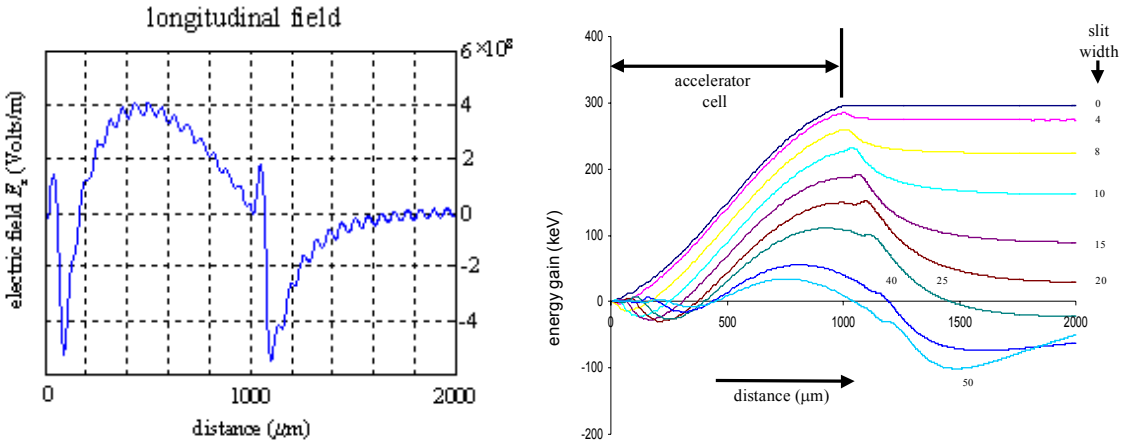

FIGURE 2: $E_z(z)$ in units of 10^8 V/m for the electron at optimal phase (left), and the energy gain in keV (right) for various slit widths, showing pronounced reduction in energy gain as the slits are opened. The entrance of the accelerator cell is at z=0 μm, the exit is at z=1000 μm.

The interaction of RF accelerator produced electron bunches with the fields calculated above is of interest for comparison with experiment. Since the proposed research will be carried out using ~5 ps FWHM electron bunches, the electrons cover all possible phases of the accelerating field, and the interaction will manifest as an energy modulation and phase bunching. Direct observation of this energy modulation forms the first phase of the proposed experimental program. Figure 3 below shows the expected energy spectra for three different slit widths, and with a laser pulse length 50 times longer than used in Figure 2. The longer pulse length is chosen to match the 5 ps long electron bunch so that

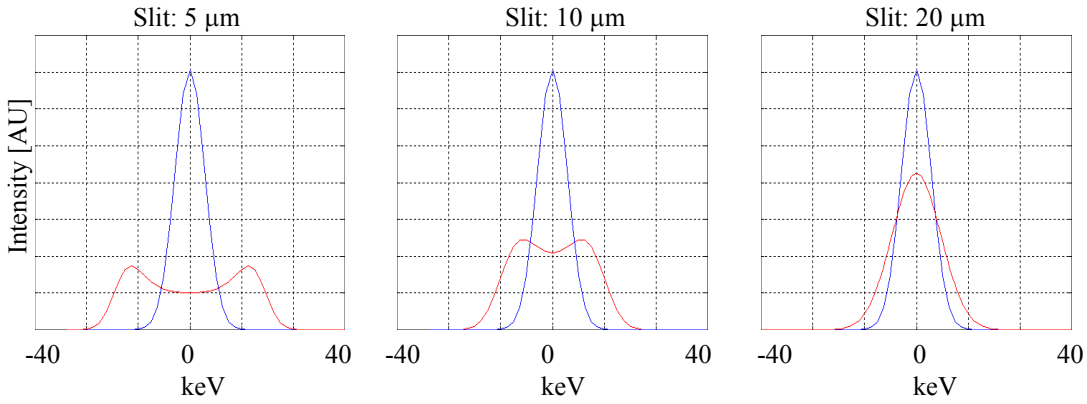

FIGURE 3: Predicted energy modulation spectra for a 5 ps electron pulse interacting with a 10 ps FWHM laser pulse for 5, 10, and 20 μm wide slits. The blue and red traces represent the electron bunch spectra before and after the laser interaction, respectively.

the entire electron bunch experiences the laser fields. The laser pulse length will be varied to maximize the acceleration gradient and electron/photon overlap, so this is a representative case only. The effects of field leakage make performing the experiment

with slits much wider than 10 μm very difficult. It is also clear that the energy spread of the probe electron beam must be quite small or the effect will not be visible.

Prior Experimental Results

Much of the experimental effort in advanced laser acceleration research has concentrated on using plasmas to couple radiation to beams, owing to the recent demonstrations of extraordinary gradients (>100 GeV/m)[8]. Although ultimate gradients achievable with vacuum laser acceleration are somewhat lower owing to the damage threshold of the material boundaries, the presence of solid boundaries and the absence of nonlinear plasma interactions offers some potential advantages in controlling the beam quality.

The experimental examination of direct laser acceleration is a very new field, made practical only within the last half decade by the commercialization of chirped-pulse-amplified lasers. Key technical accomplishments needed to make a practical laser accelerator have come only in the last year or two, with the first demonstration of phase-locking of a laser to a microwave reference, noted above, and with the development of highly efficient semiconductor lasers.

The STELLA[9] (STaged ELectron Laser Acceleration) experiment at Brookhaven's Accelerator Test Facility has achieved remarkable results working in the far-IR wavelength range. Optical bunching has been demonstrated at 10 micron wavelength using an Inverse Free Electron Laser (IFEL) as the buncher, and has been followed by a successful staging demonstration (i.e. bunching followed by acceleration) using initially an Inverse Cerenkov Accelerator second stage, and most recently a second IFEL. These landmark demonstrations have shown that bunching and manipulation of electron beams at the attosecond (10^{-18} sec) time scale is achievable and practical, without the need for extraordinary measures.

The Laser Electron Acceleration Project ("LEAP"), initially funded in 1996 by the DOE office of Advanced Accelerator R&D, was designed to make the first demonstration of linear electron acceleration in vacuum by crossed Gaussian laser beams. This experiment, working at 0.8 micron, demonstrated many of the experimental techniques required of the experiment proposed here. They range from the construction of accelerator cells with alignment tolerances in the microns, the miniaturization of beam diagnostics for inclusion in a very compact interaction region ($<(5\text{cm})^3$), the handling and diagnosing of ultra-low charge electron bunches (down to a few hundred femtoCoulombs), to the measuring of electron/photon timing at the picosecond scale by both direct (Cerenkov-radiation based diagnostic) and indirect (phase detection of beam-induced signals) methods.

To date, only tantalizing hints of the interaction signature (c.f. Figure 3) have been seen at LEAP. Significant jitter in the position and timing of the electron and laser pulses, and scant experimental run time have made observation of the signal difficult, but it is expected that with improved statistics the signature will become evident.

Context of this Research Proposal

The research program described here focuses almost entirely on understanding the laser-electron interaction, how to make efficient accelerator structures, and how to make and diagnose optically bunched beams. This effort is part of a larger program to develop each of the central technologies needed to realize a high energy laser accelerator.

The LEAP effort has been partially funded through the DOE's Advanced Accelerator Research and Development program, which is part of the broader High Energy Physics program. The original grant has been renewed, and funding will continue until 2002, when renewal will again be sought. This funding will be used to support the E-163 scientific program when the experiment is moved from its present location at the Hansen Experimental Physics Laboratory (HEPL) on Stanford Campus to SLAC.

To pursue high efficiency laser development, Prof. Byer's Center for Nonlinear Optical Materials has submitted a proposal to DARPA seeking funds to develop high-average-power mode-locked lasers with high efficiency for accelerator use. In addition, this year's DOE SBIR solicitation specifically solicited and received proposals for developing efficient 1.5-2.0 μm lasers and for lithographic fabrication of silicon and silica microstructures suitable for laser acceleration. Technology suitable for laser acceleration is expected to remain part of the SBIR solicitations in years to come.

Lithographic structure development is underway and will continue at both the Ginzton Microfabrication Laboratory and the Paul G. Allen Center for Integrated Systems (CIS) on Stanford campus. The Ginzton and CIS laboratories form a world-class nanofabrication facility for advanced optical and electron-beam lithography, semiconductor process, and analysis.

Experiment Design and Requirements

Laser acceleration experiments share the need for a powerful drive laser and specialized diagnostics for probing the properties of the required very low-charge, low-emittance beams. A low energy electron beam of 60 MeV will be produced in a radiofrequency photoinjector and preaccelerator, focused to a spot size of order 10 μm and passed through the test accelerator. A high resolution charged particle beam spectrometer, located immediately downstream of the test accelerator, will be the primary diagnostic for understanding the electron beam interaction with the test accelerator. Profile monitors and timing monitors will also be required to establish that synchronism and alignment conditions will be met.

Low charge bunches, with sufficient charge for accurate diagnosis, are desired to probe the fields of the accelerator cells. Reasonable beam quality is required, with emittances small enough that there is no appreciable beam scraping on the entrance slits of the accelerator cell, a relatively easy condition to satisfy for the low charge, high energy beams of the NLCTA. The electron bunch energy spread must be quite narrow, of order 20 keV rms, in order that (1) the initial energy modulation signature to be plainly visible and not washed out by the native energy spread of the beam, and that (2) the optical phase bunching not to wash out before acceleration can take place. These beam requirements are summarized in Table 1 on the next page.

As the accelerator cell dimensions are small, position jitter at the location of the cell will cause charge jitter after the cell, but as the accelerator cell sits at the focus of a high demagnification lens, the position jitter is largely mitigated. Temporal jitter is more serious, as the electron and laser pulses, each of order a few picoseconds in duration, must overlap. This translates into a fairly restrictive timing jitter limit between the RF and modelocked laser phases. The transport optics, together with the NLCTA chicane, may be used to partially ameliorate this jitter, by imparting a small energy chirp on the

TABLE 1: Summary of electron and laser beam parameter requirements.

Parameter	**Value**	**Comment**
Electron Beam Properties		
Bunch Charge	50 pC	
Beam Energy	60 MeV	
Transverse Emittance	< 2.5 π mm-mr	Normalized
Bunch Length	< 5 ps	FWHM
Energy Spread	< 20 keV	FWHM
Pulse Repetition Rate	10 Hz	
Laser Beam Properties (for experiment)		
Pulse Energy	1 mJ	
Pulse Wavelength	800 nm	
Pulse Length	0.1-10 ps	FWHM, variable
Pulse Repetition Rate	10 Hz	
Timing jitter w.r.t. electron beam	< 1 ps	

beam and setting the chicane and transport optics to give pulse compression, which will also compress the timing jitter.

It is expected that beam availability of 1 week per month will lead to rapid progress in each of the proposed experiments. Appreciable installation and optical setup time and data analysis is involved in each experiment, and can proceed in the time between experimental runs. The total duration of the experimental phase (excluding the installation and commissioning of modifications to the NLCTA) is expected to be 30 months.

Acceleration Test Setup at the NLCTA

Several changes to the NLCTA facility will be required to permit its use for laser acceleration experiments. First, as presently commissioned, the NLCTA injector produces pulse trains from a DC thermionic source with an average current of up to 2 amperes, and transverse emittances that are quite large, typically in excess of 100 π mm-mr. The multiple pulse structure is a problem as electron bunches in buckets other than the accelerated bucket will stack up on top of the accelerated bunch in the spectrometer, greatly reducing the signal to noise ratio. In addition, the transverse emittances and characteristic energy spread are far too large to satisfactorily complete the experiments. Consequently, we propose to replace the thermionic injector with a RF photoinjector capable of producing single electron pulses of high brightness. This injector

has been designed to support not only the E-163 proposal beam requirements, but to produce higher charge beams suitable for the NLC program in RF breakdown, and for possible future plasma acceleration experiments, for which the E-163 experimental apparatus is highly suitable.

Installation of the RF photoinjector will also require a laser room adjacent the NLCTA enclosure to house the photocathode drive laser and associated diagnostics, and an s-band RF system to be installed to power the gun.

Second, the present and near-term future usage of the NLCTA calls for RF breakdown studies to be carried out, causing the NLCTA enclosure to be inaccessible most of the time. The experiments described in this proposal will involve making frequent and prolonged access to the apparatus to make improvements. and consequently, a separate shielding enclosure that permits access to the laser acceleration experiment while the NLCTA is RF conditioning is highly desirable.

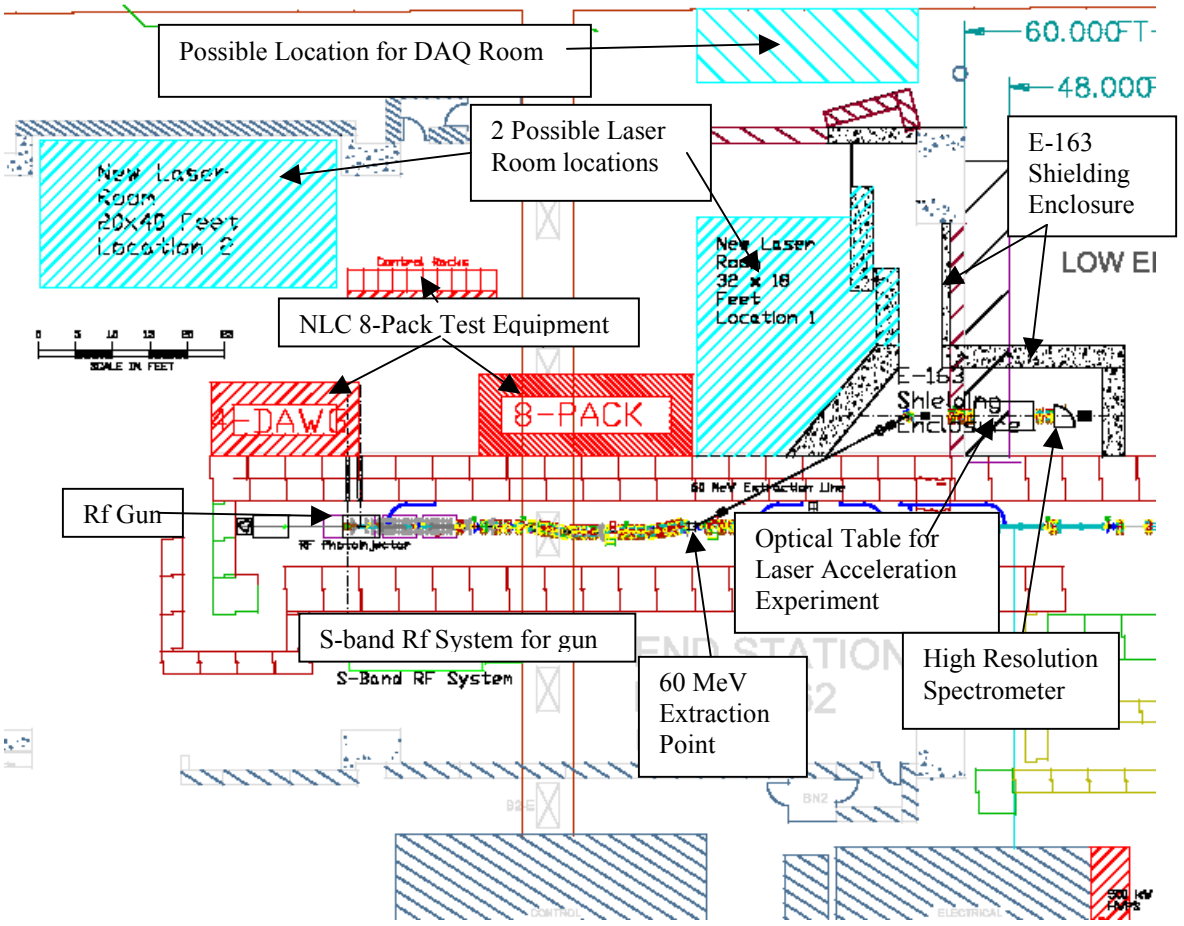

FIGURE 4: Possible layout of E-163 components in End Station B, showing two potential locations for the laser room, extraction beamline, and new shielding enclosure.

Finally, to have beam in the separate shielding enclosure, an extraction line, originating from the downstream end of the NLCTA chicane is desired, together with appropriate personnel protection systems, to transport beam from the NLCTA enclosure

to the experiment enclosure. Figure 4 below summarizes a possible layout for these components in End Station B, together with the planned 8-pack klystron test equipment.

Augmentation of the NLCTA

Replacement of the thermionic injector with a RF photoinjector will enable the NLCTA to provide a versatile range of beams for advanced accelerator research and development as well as satisfy the NLCTA program goals. An optimized s-band RF photoinjector, shown schematically in Figure 5 been designed specifically for this purpose, and the details of its construction may be found on the web at https://www-project.slac.Stanford.edu/orion/facilities/TDS.pdf. In addition to physically replacing the injector, a modest laser room of approximately 20x40 feet in size will be needed to house the photocathode drive laser. The UV light required for photoemission is produced by frequency tripling IR light, with a substantial amount of IR light remaining after the process. This remaining IR light will be spatially filtered and used to power the laser acceleration experiments.

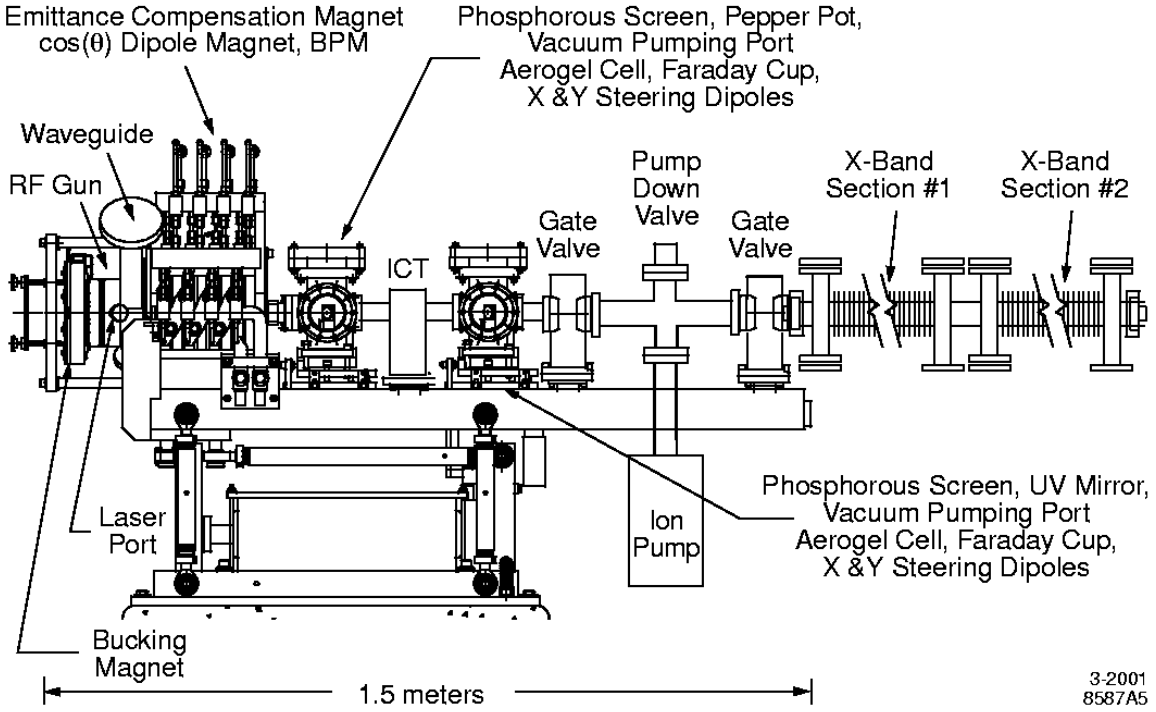

FIGURE 5: The RF photoinjector and diagnostic assembly, shown installed at the NLCTA.

Replacement of the injector is not only essential for providing the beam quality required for the proposed experiments, but will be beneficial to the NLC program. The RF photoinjector will provide, for the first time, beams of the approximate charge and emittance permitting beam transport of the high quality beams in the NLCTA to be studied, and to test the diagnostics with bunches that closely resemble those of the NLC itself.

An extraction beamline will also be needed to transport 60 MeV beam from the injector to the laser acceleration experiment. The logical choice for the pick-off point is immediately downstream of the NLCTA bunch compressor. This will permit the compressor to be used both for pulse shaping and for temporal dispersion cancellation.

The wide range of beams available from this injector not only will serve the specific goals of providing fine probe beams for laser acceleration, and high current beams for NLCTA structure probing, but can be used to accomplish a broader program of accelerator research and development. The electron source has been designed to be a flexible research tool for future accelerator R&D as well as suit the needs of E-163.

This facility has capabilities that are desirable for a broad class of acceleration experiments. An injector capable of bunch charges from a few pC to 1 nC with good emittances, good availability, and an interaction region with facilities for high-quality energy spectrometry form a facility capable of supporting many acceleration experiments.

It is anticipated that the use of this facility will extend beyond the proposed experiment. We have designed the shielding enclosure entrance labyrinth large enough to accommodate the optical table that holds the interaction chamber, and plan to install the optical table on a kinematic mount, permitting straightforward, expeditious interchange of experiments in the future.

Investigation of the Vacuum Interaction

LEAP (shown schematically in Figure 6 and in a photograph in Figure 7) has demonstrated the experimental methods for performing laser acceleration experiments, and has progressed to the point that a demonstration of the laser acceleration mechanism is possible. This demonstration of first acceleration may have already been seen in data taken in the most recent experimental runs of LEAP, but conclusive evidence, and a systematic study of the interaction character remain. Quite limited beam time and the impending renovation of HEPL in the near future make it essential to seek out a long-term alternative location with high quality beams for performing these experiments.

The installation of the LEAP experiment to ESB will allow a thorough investigation of the acceleration gradient dependence on incident laser power, slit separation, relative laser timing, and interaction length. These measurements will establish a detailed understanding of the laser driven linear acceleration mechanism, and provid information needed to engineer the next generation of structures.

The apparatus shown in Figure 7, including the vacuum systems, diagnostics for both electron and laser beams, micropositioners, spectrometer, and intensified cameras will be moved from HEPL to the NLCTA for E-163.

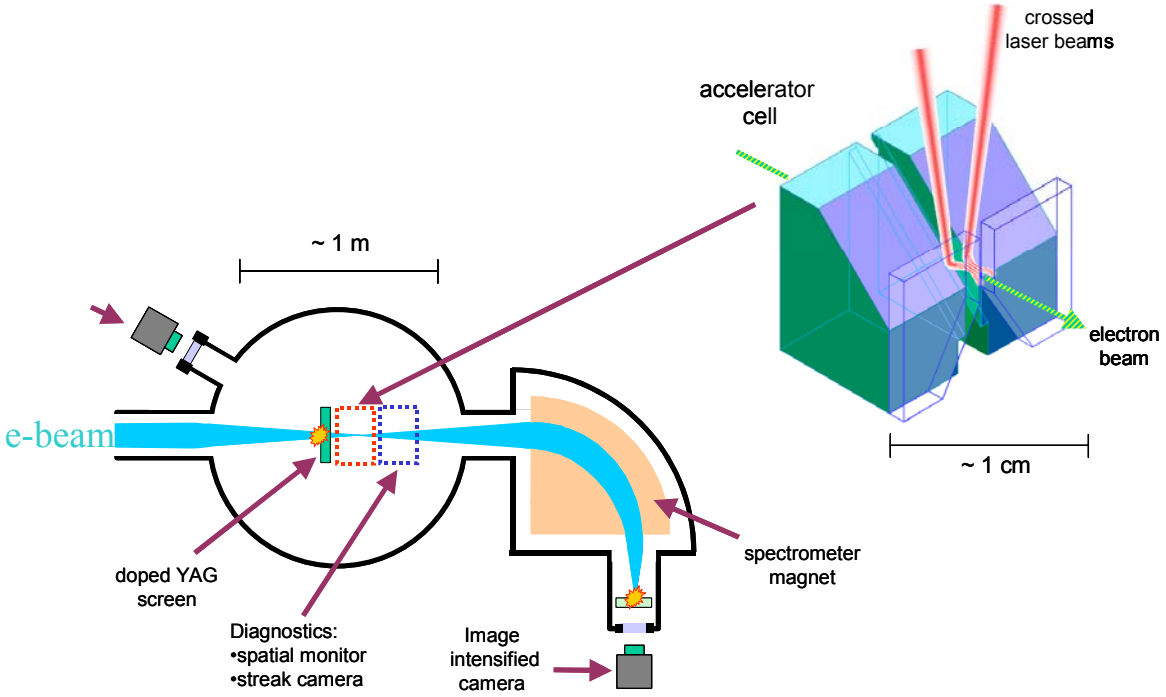

FIGURE 6: Schematic layout of the LEAP experiment.

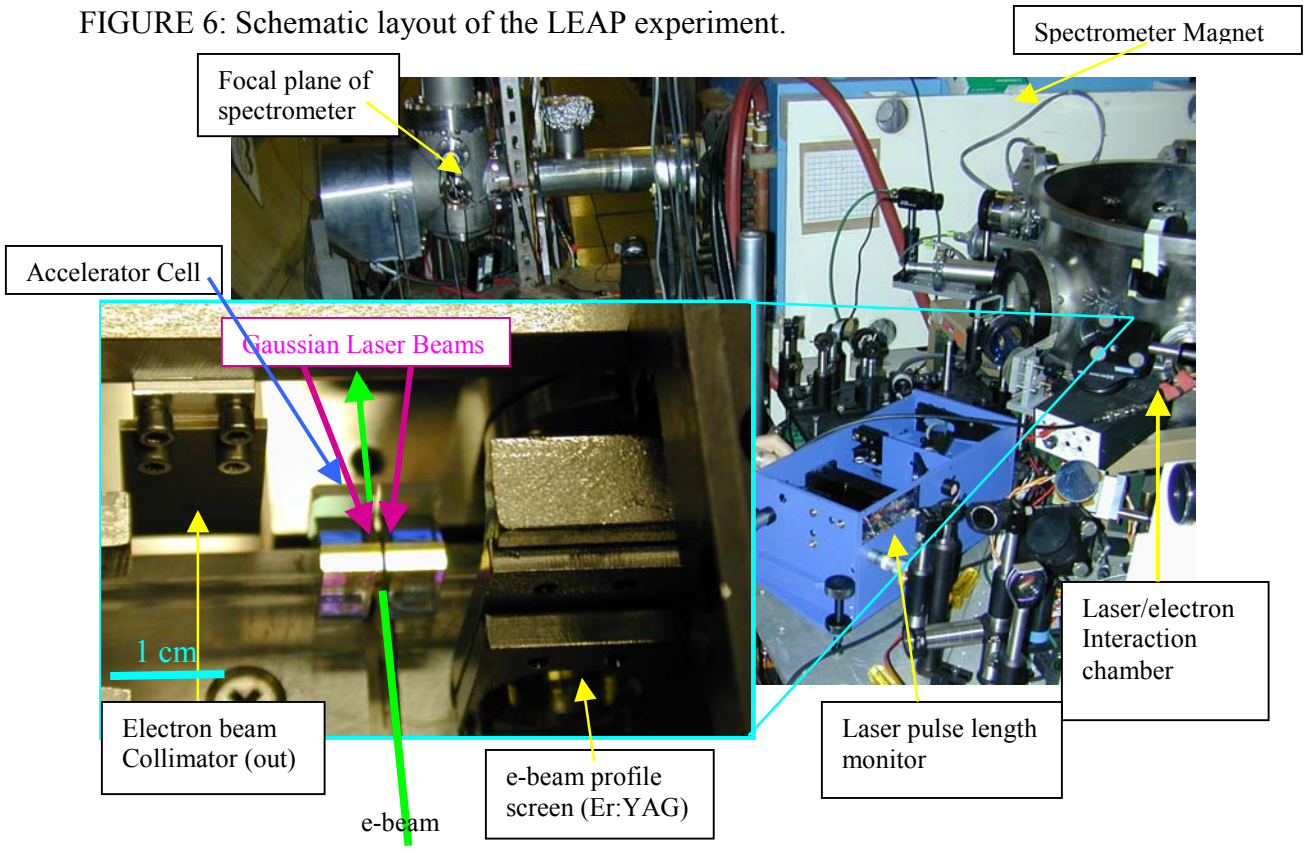

FIGURE 7: The present LEAP apparatus, showing the laser/electron interaction chamber (right), spectrometer, and spectrometer readout chamber (top left). Inset shows close-up of the accelerator cell and surrounding diagnostics.

Optical Prebunching and Acceleration

Once the interaction has been carefully characterized, the second phase is a staging demonstration. The staging setup will use an IFEL rather than a crossed-Gaussian accelerator cell to energy modulate the 5 ps long electron beam. The larger energy modulation available from the comparatively large-aperture IFEL makes bunching occur in a shorter drift distance, and makes the staging experiment both more compact and easier to commission. A short drift will allow the energy modulation to cause velocity bunching into 0.8 μm spacing optical bunches, to be followed by an accelerator cell to provide net acceleration or deceleration, depending on the relative phase of the IFEL "buncher" and the accelerator cell. By varying this relative phase, we expect to demonstrate a variation in the acceleration of the optical microbunches. As demonstrated at STELLA at 10 μm, careful attention to thermal effects, microphonics, and electron beam transport will be required to ensure that the optical bunches experience a constant phase delay from buncher to accelerator.

Figure 8 plots[10] required laser power versus wiggler length to achieve 1% peak-to-peak energy modulation on a 60 MeV beam. The laser power available from the proposed photocathode drive laser is in excess of 1 GW, permitting splitting to drive both the IFEL and an accelerator cell.

We are examining several possible ways to obtain the wiggler. We are in negotiations with STI Optronics and Boeing to use an already existing device, a spare section of the THUNDER wiggler, which has a period of 2.1 cm and is reasonably matched to our beam energy. A second possibility is to modify a wiggler we already own made by the TRW corporation, but with a 3.8 cm wiggle period it would have to be used either with lower energy electron beams, or on the third harmonic. As a third option, the SLAC klystron department is proficient at designing and manufacturing permanent magnet focussing systems, and would be a natural place to have this short, modest-tolerance

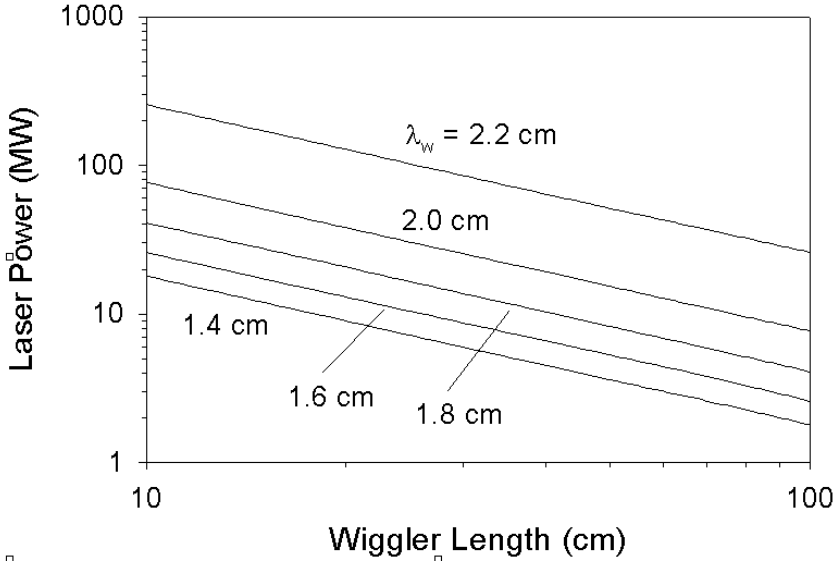

FIGURE 8: Laser power required to achieve 1% p-p energy modulation depth on 60 MeV beam as a function of total wiggler length. Undulator length and Rayleigh range are matched.

wiggler constructed.

With the successful commissioning of an optical prebuncher, we would then have an optically bunched probe "macropulse" (lasting 5 ps, it would be composed of almost 2000 optical microbunches) suitable for injection into laser accelerator structures. Wakefield studies of candidate accelerator structures would also be possible for the first time and optical bunching diagnostics (such as coherent transition radiators) could also be tested.

Accelerating Microstructures

Power efficiency and sustained energy gain will require that many accelerator cells be combined in a linear phased array, as with multicell microwave accelerating structures. In addition, to enhance efficiency, the laser power can be recycled by, for example, embedding the accelerator structure in a resonant ring structure. Current microfabrication techniques are capable of producing the small, complex structures needed for efficient acceleration. Microfabrication techniques also offer inexpensive, reliable manufacturing to high tolerance, and the economic scalability needed for mass production.

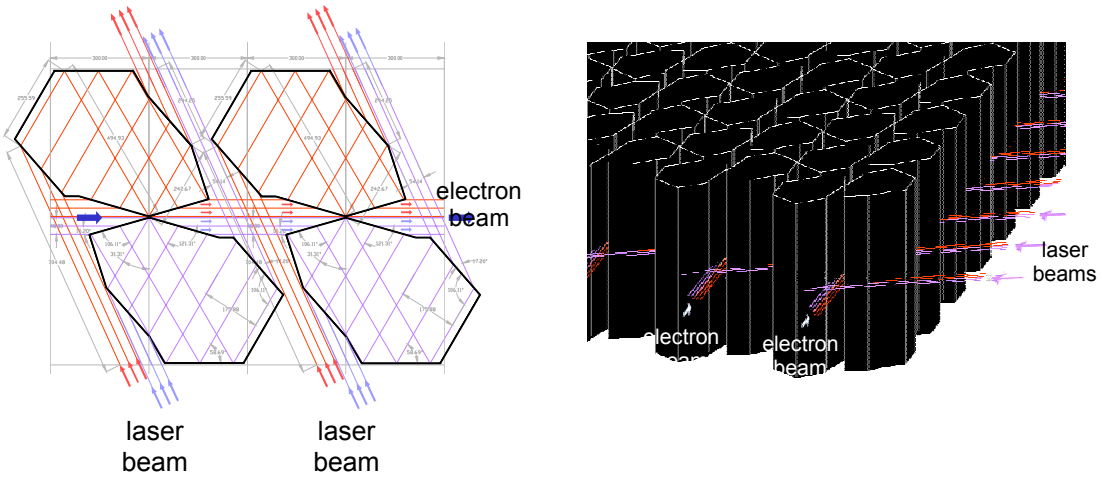

FIGURE 9: One concept for a lithographically-produced transmission-mode laser acceleration structure. On the left, a unit cell of the accelerating structure, using TEM_{10} mode beams to develop axial fields over a ~1 mm gap by total internal reflection within the substrate. Right: This cell repeated to form an acceleration structure.

Numerous ideas already exist for accelerating microstructures, including cascaded crossed-beam structures, as shown in Figure 9, and periodic lenslet waveguides, but no experimental tests have yet been done with these structures. A facility with beam frequently available will allow rapid evaluation of different structures. The third phase of this proposal will involve the production and testing of candidate multicell accelerating structures.

Request to SLAC

The Stanford University/SLAC collaboration will provide many of the experiment's central components, including the laser interaction vacuum chamber and associated diagnostics and instrumentation, some beamline magnets, the laser oscillator, the high-resolution spectrometer magnet. We request modifications to the NLCTA and the construction of the facility for laser acceleration experiments described in this proposal.

We anticipate an installation and commissioning period lasting approximately 1 year from the date of approval. Upon completion of the NLCTA modifications we request 1 week per month of beam time from the NLCTA injector for a duration of 30 months.

Future Potential

This proposal builds on the collaboration between two groups with expertise spanning lasers, electro-optics, lithography, and accelerator physics. The potential for this collaboration to make a significant impact rests on broad expertise, direct experience conducting the LEAP experiments, and the largely unexplored status of this approach to acceleration. It is expected that new concepts for laser-driven accelerators will emerge. We fully anticipate making further proposals to the EPAC for such work.

Our vision of a lithographically-produced laser-driven accelerator combines the strength of the laser to produce extraordinary electric fields, modern lithographic techniques to produce complex dielectric structures, and large markets to drive innovation and cost reduction. E-163 is the next of many steps required to make concepts like this a reality.

References

[1] M. Bellini, T. Hänsch, Opt. Lett. **25**, 1049 (2000).
[2] Diddams *et al*, Phys. Rev. Lett., **84** (22) 5102, (2000).
[3] J. Opt. Soc. Am. B, **18** (7), p. 926, July (2001).
[4] Opt. Lett., **25** (15), p.1119, August (2000).
[5] Opt. Lett., **22** (17), p.1317, September (1997).
[6] R. H. Pantell, M. A. Piestrup, Appl. Phys. Lett., **32**(11), p. 781-3, (1978).
[7] C. M. Haarland, Opt. Comm. **114**, p.280m (1995).
[8] W. P. Leemans, E. Esarey, AIP Conf. Proc. 472, (1998).
[9] M. Babzien, *et al*, AIP Conf. Proc. **569**, p. 146, (2001).
[10] W. Kimura, personal communication, (2001).

Appendix A: Accelerator Field Calculations

Three calculation methods have been developed for evaluating the fields and beam dynamics for the crossed-Gaussian accelerator cell. A compact analytic description is possible only for an accelerator cell with no openings for the electron beam to pass, but already exhibits many of the dependencies of the fields and particle dynamics on the cell geometry. Two numerical treatments augment this simple theory, the first based on decomposing the incoming Gaussian beam modes as a set of paraxial plane waves, propagating, then summing to obtain the fields in the cell (producing Figure 1 in the main text), the second based on a more cumbersome but complete vector diffraction treatment.

Analytic Theory

The fields of a single linearly polarized TEM_{00} beam propagating at an angle θ to the electron beam, given in the electron beam's Cartesian coordinates are (reproduced from Sprangle *et al*[1]):

$$E_x = E_o \frac{w_o}{w_1} \exp(-r_1^{\,2} / w_1^{\,2}) \cos\psi_1$$
$$E_z = 2E_o \frac{x_1}{k w_1^{\,2}} \exp(-r_1^2 / w_1^2) \times (\sin\psi_1 - (z/z_R)\cos\psi_1) \quad (1)$$

with $w_1=w_o[1+(z_1/z_R)^2]^{1/2}$ the laser spot size, w_o the focused spot size, $z_R=\pi w_o^2/\lambda$ is the Rayleigh range, $r_1^2=x_1^2+y_1^2$, $\psi=kz_1-\omega t+\phi_1+\phi_o$, $\phi_1=r_1^2(z_1/z_R)/w_1^2-\tan^{-1}(z_1/z_R)$ is the near-field phase advance, and ϕ_o is an arbitrary phase. The off-axis wave vector is essential to the development of an axial field component to couple to the electron beam, while interacting the laser with the electron beam near the focus is essential for obtaining the highest acceleration fields.

With the addition of a second laser pulse π out of phase with the first, propagating at an angle –θ to the electron beam, the sum fields are:

$$Ex(z,t) = 0$$
$$Ez(z,t) = \frac{-2E_o \sin\theta}{(1+\tilde{z}^2\cos^2\theta)^{3/2}} \exp\left(\frac{-(\tilde{z}/\theta_d)^2 \sin^2\theta}{1+\tilde{z}^2\cos^2\theta}\right) \times (\cos\psi + \tilde{z}\cos\theta\sin\psi) \quad (2)$$

with

$$\psi = kz_R\tilde{z}\cos\theta - \omega t + \theta_d^{\,-2} \frac{(\tilde{z}\cos\theta)^3 \tan^2\theta}{1+\tilde{z}^2\cos^2\theta} - \tan^{-1}(\tilde{z}\cos\theta) + \phi_o \quad (3)$$

with the diffraction angle $\theta_d = w_o / z_R$ having been defined, and z normalized in Rayleigh ranges, $\tilde{z} = z / z_R$.

For small crossing angles, θ«1, an electron traversing these fields at approximately the speed of light experiences an axial field:

$$E_z \approx \frac{-2E_o\theta}{1+\tilde{z}^2} \exp\left(\frac{-\tilde{z}^2(\theta/\theta_d)^2}{1+\tilde{z}^2}\right)\cos\psi_t \quad (4)$$

with

$$\psi_t \approx -(\gamma\theta_d)^{-2}\tilde{z} - (\theta/\theta_d)^2\tilde{z}/(1+\tilde{z}^2) - 2\tan^{-1}\tilde{z} + \phi_o \quad (5)$$

The phase velocity of this axial field is greater than the speed of light, and thus the interaction length must be limited to provide a net energy gain. The slippage distance over which and electron beam of energy γ phase slips by π is:

$$z_s = \frac{\gamma_c^2\lambda}{1+\gamma_c^2/\gamma^2} \quad (6)$$

where the critical energy, $\gamma_c=(\theta^2+2\theta_d^2)^{-1/2}$, defines a threshold below which slippage is dominated by the difference in velocity between electrons and photons and above which slippage is dominated by diffraction. This slippage length sets the interaction length for practical accelerator cell design.

The maximum energy gain for an optimized accelerator cell used to accelerate beam above the critical energy γ_c is:

$$\Delta W = \frac{8eE_o}{k\theta}\sin\left(\frac{(\theta/\theta_d)^2\hat{z}}{1+\hat{z}^2}\right)\exp\left(-\frac{(\theta/\theta_d)^2\hat{z}^2}{1+\hat{z}^2}\right) \quad (7)$$

with $\hat{z} = z_s/(2z_R)$ the normalized ideal accelerator length.

For parameters of interest for the future, summarized in Table A.1 below, and consistent with the known[2] damage threshold value on fused silica of 2 J/cm^2, a net energy gain of 290 keV per accelerating cell is expected.

TABLE A.1: Summary of crossed-Gaussian laser and field parameters.

Parameter	**Symbol**	**Value**	**Comment**
Electron Energy	E_e	60 MeV	
Laser Wavelength	λ	0.8 μm	
Laser focal spot size	w_o	50 λ	
Rayleigh Range	z_R	6.3 mm	
Slippage Length	z_s	2.8 mm	
Ideal Crossing Angle	θ	11.5 mrad	
Critical Energy	γ_c	68	(34 MeV)
Spot size on dielectric surface	w_1	51.3 λ	
Fluence x time on dielectric surface	$F\cdot\Gamma_t$	2 J/cm^2	
Laser Pulse Energy	E_γ	100 μJ	
Laser Pulse Length	Γ_t	100 fsec	FWHM
Peak Electric Field	E_o	5.9 GV/m	
Peak Axial Field	E_z	140 MV/m	
Energy Gain	ΔW	290 keV	Ideal phase particle

Plane Wave Decomposition

This simple model does not include the effects of opening a slit for the electron beam to pass, and consequently, real acceleration cell design requires a numerical model. A numerical code was written to express the Gaussian beams in a plane wave decomposition following Edighoffer and Pantell[3]. The fields of the incident Gaussian

pulses polarized in the x-z plane may be expressed as an infinite sum of plane waves propagating in the z-direction with an associated angular spectrum:

$$E_{0x} = \int_{-\pi/2}^{\pi/2}\int_{-\pi/2}^{\pi/2} A_0(\alpha,\beta)\cos\alpha\exp(i(k\cdot x\cos\beta\sin\alpha + k\cdot y\sin\beta))d\alpha d\beta$$
$$E_{0z} = \int_{-\pi/2}^{\pi/2}\int_{-\pi/2}^{\pi/2} A_0(\alpha,\beta)\sin\alpha\exp(i(k\cdot x\cos\beta\sin\alpha + k\cdot y\sin\beta))d\alpha d\beta \quad (8)$$

in which α is the angle of propagation w.r.t. the z-direction in the x-z plane and β is the angle of propagation in the rotated y-z plane, w.r.t. the rotated z-direction.

In the paraxial approximation ($\alpha,\beta \ll 1$) small angle approximations for the trigonometric functions may be used, and the integration limits extended to infinity, yielding:

$$E_{0x} \approx \int_{-\infty}^{\infty}\int_{-\infty}^{\infty} A_0(\alpha,\beta)\exp(i(k\cdot x\alpha + k\cdot y\beta))d\alpha d\beta$$
$$E_{0z} \approx \int_{-\infty}^{\infty}\int_{-\infty}^{\infty} A_0(\alpha,\beta)\cdot\alpha\cdot\exp(i(k\cdot x\alpha + k\cdot y\beta))d\alpha d\beta \quad (9)$$

where equation (9a) is just the Fourier transform of the spectral function A_o. Since the transverse field component is much larger than the longitudinal component, it is a good approximation to evaluate the spectral function directly from the inverse Fourier transform of the transverse field distribution on the source plane:

$$A_0 \approx \frac{1}{\lambda^2}\int_{-\infty}^{\infty}\int_{-\infty}^{\infty} E_x(x,y)\exp(-i(k\cdot x\alpha + k\cdot y\beta))dxdy \quad (10)$$

With the source spectral function known, the spectral function may be propagated to field points in the image plane:

$$A_i(x,y,z) = A_0\exp(ikz\sqrt{1-\cos^2\beta\sin^2\alpha - \sin^2\beta}) \approx A_0\exp(ikz(1-\tfrac{1}{2}\alpha^2 - \tfrac{1}{2}\beta^2)) \quad (11)$$

and the fields evaluated using:

$$E_{ix} \approx \int_{-\infty}^{\infty}\int_{-\infty}^{\infty} A_0(\alpha,\beta)\cdot\exp(ikz(1-\tfrac{1}{2}\alpha^2 - \tfrac{1}{2}\beta^2))\cdot\exp(i(k\cdot x\alpha + k\cdot y\beta))d\alpha d\beta$$
$$E_{iz} \approx \int_{-\infty}^{\infty}\int_{-\infty}^{\infty} A_0(\alpha,\beta)\cdot\exp(ikz(1-\tfrac{1}{2}\alpha^2 - \tfrac{1}{2}\beta^2))\cdot\alpha\cdot\exp(i(k\cdot x\alpha + k\cdot y\beta))d\alpha d\beta \quad (12)$$

The phase slippage of the electrons must be accounted for by adding a simple phase correction factor to the fields:

$$E_{ix} \to E_{ix}\cdot\exp(-ikz/\overline{\beta})$$
$$E_{iz} \to E_{iz}\cdot\exp(-ikz/\overline{\beta}) \quad (13)$$

where $\overline{\beta}$ is electron velocity in units of c.

The numerical simulation replaces the Fourier integral of equation (10) by a discrete sum over a spatial area in the source plane that is large compared to both the wavelength and the mode size. The integrals in equation (13) are similarly replaced by discrete sums over a narrow angular range that is large compared to the maximum beam divergence seen in the focal region. The energy change of an electron traversing these fields is

evaluated in the Born approximation (i.e. assuming no trajectory change due to the interaction) by integrating the on-axis longitudinal field:

$$U(z,\phi) = \Re e\{\exp(i\phi_o)\int_0^z E_{iz}(z')dz'\} \tag{14}$$

where the arbitrary phase ϕ_o accounts for the timing of the electron's entry into the optical field. The effect of the entrance slit is approximated by setting $E_x(x,y)$ to zero everywhere within the slit region on the source plane prior to evaluating equation (10).

Vector Diffraction

It is interesting to note that the acceleration cell has dimensions which are ~10^3 λ, with scattering features (the slits) ~10^1 λ in extent. This places the description and design of such cells squarely in the quasioptical domain, a regime well known to radar antenna engineers. More importantly, this also means that despite the small dimensions of these optical structures, they are much longer and much more open than their microwave counterparts. Were the accelerator cell above scaled to the same wavelength as the SLAC linac, the interaction length would be nearly 350 meters, and the slit gap separation would be nearly 1.3 meters, far larger and far more open than the typical s-band guided mode structure!

Drawing on antenna engineering experience[4], a 3D vector diffraction code has been written to permit detailed models of both reflective and transmissive geometries to be evaluated with non-ideal surface impedance characteristics fully accounted for. The basic computational method is an implementation of Huygen's principle with incoming optical modes approximated as a set of equivalent discrete electric and magnetic dipoles on a source plane, and propagated exactly to field planes. Surface interaction is via computation of equivalent induced currents on the field surface using the surface's impedance, then re-radiating to the next set of field points. This method is ideally suited to problems of this type, provided there are only a small number of reflections to be accounted for.

It is fully anticipated that commercial codes intended for the design of antennas, fiber optics, and waveguiding systems will soon be suitable for this class of problems. Many codes already exist which calculate scattering parameters for optical devices with geometries similar to those we propose to test. What is not available are codes which provide the computed fields themselves, information essential for designing accelerators.

References

[1] R. H. Pantell, M. A. Piestrup, Appl. Phys. Lett., **32** (11), p.781, (1978).
[2] M. D. Perry, *et al*, J. Appl. Phys., **65** (9), p.6803, (1999).
[3] J. A. Edighoffer, R. H. Pantell, J. Appl. Phys., **50** (10), p.6120, (1979).
[4] L. Diaz, T. Milligan, "Antenna Engineering Using Physical Optics: Practical CAD Techniques and Software", (Boston: Artech House, 1996).